HHS Public Access

Author manuscript

Insect Biochem Mol Biol. Author manuscript; available in PMC 2015 July 01.

Published in final edited form as:

Insect Biochem Mol Biol. 2015 July ; 62: 11–22. doi:10.1016/j.ibmb.2014.08.006.

Identification and profiling of *Manduca sexta* microRNAs and their possible roles in regulating specific transcripts in fat body, hemocytes, and midgut ☆

Xiufeng Zhang[1], **Yun Zheng**[2], **Xiaolong Cao**[1,3], **Ren Ren**[4], **Xiao-Qiang Yu**[5], and **Haobo Jiang**[1,*]

Xiufeng Zhang: xiufeng.zhang@okstate.edu; Yun Zheng: zhengyun5488@gmail.com; Xiaolong Cao: xiaolong.cao@okstate.edu; Ren Ren: renren@fudan.edu.cn; Xiao-Qiang Yu: yux@umkc.edu; Haobo Jiang: haobo.jiang@okstate.edu

[1]Department of Entomology and Plant Pathology, Oklahoma State University, Stillwater, OK 74078, USA

[2]Faculty of Life Science and Technology, Kunming University of Science and Technology, Kunming, Yunnan 650500, P.R. China

[3]Department of Biochemistry and Molecular Biology, Oklahoma State University, Stillwater, OK 74078, USA

[4]School of Life Sciences, Fudan University, Shanghai 200433, P.R. China

[5]Division of Molecular Biology and Biochemistry, University of Missouri-Kansas City, Kansas City, MO 64110, USA

Abstract

Significance of microRNA-mediated posttranscriptional regulation has been appreciated ever since its discovery. In the tobacco hornworm *Manduca sexta*, 164 conserved and 16 novel microRNAs have been identified experimentally (Zhang et al., 2012, 2014). To extend the list of microRNAs in this lepidopteran model species and further explore their possible regulatory roles, we constructed and sequenced small RNA libraries of *M. sexta* fat body, hemocytes and midgut, since transcriptomes of these tissues from the 5th instar larvae had been studied quite extensively. Each library represented a mixture of the same tissues from larvae that were naïve or induced by three different pathogens. From a total of 167 million reads obtained, we identified two new variants of conserved miR-281 and miR-305 and six novel microRNAs. Abundances of all microRNAs were normalized and compared to reveal their differential expression in these three tissues. Star strands of ten microRNAs were present at higher levels than the corresponding mature strands. From a list of tissue-specific transcripts, we predicted target sites in 3′-UTRs using preferentially expressed microRNA groups in each tissue and suggested possible regulatory roles of these microRNAs in energy metabolism, insecticide resistance, and some mitochondrial and immune gene expression. Examining manifold targets, microRNA regulations were suggested of

☆While microRNA

Send correspondence to: Haobo Jiang, Department of Entomology and Plant Pathology, Oklahoma State University, Stillwater, OK 74078, Telephone: (405)-744-9400, Fax: (405)-744-6039, haobo.jiang@okstate.edu.

*naming is still used, their corresponding -5p or -3p names are posted on our website (http://entoplp.okstate.edu/profiles/profiles/jiang.htm).

multiple physiological processes. This study has enriched our knowledge of *M. sexta* microRNAs and how microRNAs potentially coordinate different physiological processes.

Keywords

innate immunity; insecticide toxicity; metabolism; mitochondrial miRNA regulation; target site prediction; Illumina sequencing

1. Introduction

MicroRNAs (*i.e.* miRNAs), about 22 nt long, post-transcriptionally regulate their target mRNAs. Derived from direct transcripts or intron lariats, miRNA precursors exhibit canonical stem-loop secondary structures (Asgari, 2011). Upon Dicer-1 cleavage, one strand of the miRNA duplex (miRNA:miRNA*) is loaded into RISC to bind its target (typically in 3′-UTR of the mRNA) and executes translational repression or mRNA degradation. The passenger strand miRNA*s usually exist at levels much lower than their corresponding mature strands, some hardly detectable by deep sequencing. Under some circumstances, miRNA*s are maintained at higher levels indicative of potential roles in regulating other genes (Etebari et al., 2013; Zhang et al., 2014). The dominant usage of either 5p- or 3p-arms of miRNA precursors displays lineage specificity implying a possible miRNA evolution mechanism (Marco et al., 2010) and is closely associated with the physiological status of a specific tissue (Li et al., 2012b). In the past decades, miRNAs are found to participate in the regulation of various physiological processes including development, host defense, metabolism, and stress responses (Asgari, 2011; Baker and Thummel, 2007; Chawla and Sokol, 2011).

In insects, most miRNA studies are focused on development, tissue differentiation, and miRNA biogenesis. Recent research uncovered miRNA regulation in defense against viruses, bacteria, fungi, and apicomplexan parasites (Asgari, 2011; Hakimi and Cannella, 2011; Zhang et al., 2014). Although metabolites were suggested to mediate insect immune reactions (Stanley et al., 2009) and metabolism is essential to insect homeostasis, little is known on how miRNAs may regulate insect metabolic processes. Hypometabolism is a common strategy of insects to avoid environmental stresses like freezing and starvation. Possible regulatory pairs were suggested of miRNAs and enzymes in the fatty acid biosynthesis and degradation pathways based on evidence from natural models other than insects (Lyons et al., 2013a). Dysregulated miRNAs were identified in the goldenrod gall fly *Eurosta solidaginis* during freezing and in the red flour beetle *Tribolium castaneum* upon starvation, which were potentially linked to hypometabolism (Courteau et al., 2012; Freitak et al., 2012; Lyons et al., 2013b). However, it is unclear what targets those miRNAs might recognize. In *Drosophila*, several miRNAs (miR-8, -14, -33 and -278) modulate the balance of insulin signaling pathway and lipid storage (Baker and Thummel, 2007; Davalos et al., 2011; Hyun et al., 2009). Still, lipid metabolism is the only process examined; more information is needed to fully appreciate miRNA regulation of metabolism of carbohydrates, amino acids, and others. Intriguingly, miR-8 was also found to regulate antimicrobial peptide production in *D. melanogaster* and *Plutella xylostella* (Choi and Hyun, 2012;

Etebari and Asgari, 2013). By examining manifold targets of one miRNA, it is possible to discover more miRNA regulatory correlations between immunity and metabolism in insects.

The tobacco hornworm, *Manduca sexta*, has been utilized as a biochemical model to study insect physiological processes, like hormonal control, innate immunity, cuticle formation, and neural development (Hiruma and Riddiford, 2010). Fat body and hemocytes are major sources of plasma proteins while fat body and midgut are crucial for metabolism. *M. sexta* fat body and hemocytes have been extensively investigated to understand their roles in immune responses upon bacteria injection into the 5^{th} instar larvae. The quantitative transcriptome studies of fat body and hemocytes have uncovered differentially expressed proteins likely involved in immunity (Gunaratna and Jiang, 2013; Zhang et al., 2011; Zou et al., 2008). The analysis of *M. sexta* midgut transcriptome revealed enzymes involved in digestion, detoxification and immunity (Pauchet et al., 2010). With the genome sequence available, more transcripts will be examined to facilitate future research on *M. sexta* fat body, hemocytes and midgut. Our recent study reported miRNA profiles in *M. sexta* fat body and hemocytes with or without pathogen stimulation and suggested potential regulatory pairs of miRNAs and immunity-related genes (Zhang et al., 2014). Sequencing the tissue RNAs yielded better coverage of the miRNA repertoire than the whole body samples (Zhang et al., 2012). However, tissue specificity of miRNA expression has not yet been explored in fat body or hemocytes. Neither is information available on how miRNAs may regulate *M. sexta* metabolic processes or if some miRNAs co-regulate metabolism and immunity.

Therefore, we attempted to identify more miRNAs, examine tissue-preferential expression of miRNAs and, more importantly, discover possible miRNA coordination of metabolism and systematic immune responses. To achieve these goals, we constructed small RNA libraries of larval fat body, hemocytes and midgut. Each library represented the same tissue in four immune states. For instance, the fat body library was built using a pool of the tissue samples from naïve and induced larvae separately injected with *Escherichia coli*, *Bacillus subtilis*, and *Saccharomyces cerevisiae*. Normalized miRNA abundances were compared and categorized into the three tissue groups. For each group, we identified the transcripts specifically expressed in that tissue of the 5^{th} instar larvae and predicted the target sites in their 3′-UTRs. The combined analysis of miRNA profiles and mRNA tissue-specificity allowed us to discover potential regulatory relationships at the tissue level in terms of metabolism and immunity. By including midgut tissue samples, pooling tissues in various physiological states, and increasing throughput of sequencing, we obtained an extensive list of conserved and novel miRNAs to complement the *M. sexta* genome project.

2. Materials and Methods

2.1. Sample preparation and Illumina sequencing

Three groups of *M. sexta* larvae (day 2, 5^{th} instar, six in each group) were injected with heat-killed *E. coli* (5×10^7 cells/larva), *Bacillus subtilis* (5×10^7 cells/larva) and *Saccharomyces cerevisiae* (1×10^7 cells/larva), respectively. After 6 h, hemolymph was collected and centrifuged at 5000*g* for 5 min to harvest hemocytes. The larvae were subsequently dissected for fat body and midgut tissues. Hemocytes, fat body and midgut tissues were

obtained in the same way from six day 3, 5th instar naïve larvae. The three tissue pools were separately ground in liquid nitrogen and stored in TRIZOL Reagent (Thermo Fisher Scientific) at -80°C prior to shipping on dry ice. The small RNA libraries of hemocytes, fat body and midgut were constructed at BGI (Beijing, China) and sequenced using Illumina technology.

2.2. Identification of conserved and novel miRNAs and miRNA profiling

Sequence analyses were performed as described previously (Zhang et al., 2012). Briefly, small RNAs without perfect match to the 3′-adaptor were disposed. Reads were further removed if they resemble repeats, noncoding RNAs (*e.g.* rRNAs, tRNAs, snRNAs) or mitochondrial RNAs in the respective online databases. Possible mRNA degradation products were filtered out by comparing them with the CIFH dataset (Gunaratna and Jiang, 2013; Zhang et al., 2011; Zou et al., 2008), midgut EST dataset (Pauchet et al., 2010), and Cufflink RNA-Seq Assembly 1.0 (http://agripestbase.org/manduca/). Conserved miRNAs were selected according to miRBase (v20, http://www.miRBase.org/). Their loci were obtained by retrieving mature miRNA sequences in *M. sexta* Genome Assembly 1.0 (http://agripestbase.org/manduca/). Corresponding precursor sequences were identified if they had ≥18 matched base pairs, a single central loop, and minimum free energy (MFE) < -18 kCal/mol (http://mfold.rit.albany.edu/?q=mfold/RNA-Folding-Form2.3) (Zuker, 2003). Novel miRNA mature sequences were designated based on the following criteria: ≥10 total reads in the three libraries combined, ≤5 genomic loci, precursors identified similarly as the conserved miRNAs, highest abundances compared to other reads mapped to the precursors, and existence of predicted miRNA* strands. The ones without accompanying miRNA* strands are considered to be novel miRNA candidates. Normalized frequencies for both conserved and novel miRNAs were calculated based on the size of each small RNA library. Heat maps of normalized miRNA counts were generated using Multiexperiment Viewer (v4.9) (Saeed et al., 2003). Log_2NC values (NC for normalized count) were actually used as data input. If an NC < 0.5, $log_2$0.5 was taken to represent the low miRNA abundance. Figure of Merit (FOM) was plotted to determine an appropriate number of K-means clusters with Pearson correlation. Pearson correlation and K-means clustering with maximum iterations of 50,000 were chosen for creating the heat maps. Color scale limits were set at 0 for low (blue) and at 22.1 for high (red), where 22.1 was the highest log_2NC value in the dataset.

2.3. Detection of tissue-specific transcripts in M. sexta fat body and midgut

Specific transcripts were selected based on results from analysis of the 52 RNA-Seq datasets corresponding to different tissues and stages of *M. sexta* (Cao et al., unpublished data). Briefly, reads from all these datasets were first assembled using Trinity (Grabherr et al., 2011) and FPKMs were calculated by RSEM (Li and Dewey, 2011). Due to sampling differences, the datasets of fat body and midgut from day 1, 5th instar larvae were used to calculate transcript levels, detect tissue specific expression, and correlate with miRNA levels, since this stage is the closest to that used for constructing the three small RNA libraries. Ratio for a specific transcript was calculated using its FPKM in the fat body or midgut dataset over its average FPKM in datasets excluding the same tissue. Initial screens for tissue-specific transcripts were performed under the following conditions: transcript length >300 nt, FPKM >15 (for fat body) and 25 (for midgut), ratio >3, and log_{10}(ratio)

×$\log_{10}$(FPKM in the two datasets) >1. Redundant transcripts were removed if they are >90% similar in sequence, their translated protein sequences are <80 residues, or transcripts have no 3′-UTRs. Proteins encoded by the remaining transcripts were used as queries to perform BLASTP search of uniprotKB_Arthropoda (ftp://ftp.ebi.ac.uk/pub/databases/fastafiles/uniprot/uniprotkb_arthropoda.gz). Transcripts that had no hit or only hit uncharacterized proteins were no longer analyzed.

2.4. miRNA target site analysis

The fat body- and midgut-specific transcripts were selected for target site prediction, along with the eleven hemocyte-specific transcripts (Zhang et al., 2011). 3′-UTRs were collected for *M. sexta* miRNA target site analysis using *Hitsensor* (Zheng and Zhang, 2010).

3. Results

3.1. Overview of the dataset

From the three small RNA libraries, we in total obtained ∼167 million reads, far exceeding the 21.1 and 32.9 million in our previous datasets (Zhang et al., 2012), (Zhang et al., 2014). BGI proprietary technologies of small RNA library construction and sequencing apparently led to the differences. The previous studies retrieved small RNAs in the range of 18-31 nt, whereas the current one recovered reads of 18-44 nt in length (Fig. 1), in spite of low counts for reads longer than 31 nt. The new dataset comprised higher percentages of noncoding RNAs, miRBase precursors, hemocyte-fat body-midgut ESTs, Cufflink transcripts, repeats, and Genome Assembly 1.0 (Table 1). However, in terms of the unique read percentages for each library, they were similar to the dataset of *M. sexta* CIFH small RNAs (Zhang et al., 2014) in the categories of noncoding RNAs, miRBase precursors, and repeats. Compared with hemocytes, fat body and midgut had higher percentages of unique reads matching hemocyte-fat body-midgut ESTs, Cufflink transcripts, and Genome Assembly 1.0. Since reads were removed if they matched noncoding RNAs, mRNA fragments and repeats, the differences should not adversely affect miRNA identification or profiling. The ratios of total counts over unique counts, representing miRNA average abundances, were 693, 988, and 188 for fat body, hemocytes and midgut, respectively, much higher than those of CF (56), IF (51), CH (85) and IH (79) (Zhang et al., 2014).

3.2. Identification of additional M. sexta miRNAs

We have identified another six novel miRNAs, one of which, t4742895, was present at much higher levels (Table 2). Their corresponding precursors could form canonical stem-loop structures with MFE lower than -18 kcal/mol (Fig. 2 and Table 2). t357780, t454580, t2290056 and t3057689 were at low levels and it might be possible that those four miRNAs were not preferentially expressed in the three selected tissues at the specific sampling time. Due to the failure of detecting their corresponding star strands, t357780, t454580, t3057689 and t3301296 were reported as novel miRNA candidates (Zhang et al., 2014), while t4742895 was reported as s856646 (Zhang et al., 2012). These five candidates were present at extremely low levels in the old datasets. The most dramatic example was s856646 or t4742895, whose read numbers in the whole body libraries of embryos (20), larvae (9), pupae (11) and adults (32) were much lower than those in the 5th instar larval fat body

(131,975), hemocytes (66,051) and midgut (41,738). Due to spatiotemporal specificity of miRNA expression, more candidates are expected to be advanced to novel miRNAs in future small RNA library sequencing projects covering other tissues or time points. Here we present another 26 novel miRNA candidates (Table S1). Among them, small RNAs t6322016 and t3125494 may be derived from two precursors, and the two precursors of t6322016 arose from convergent templates at the same genomic loci, rendered as antisense miRNA candidates. Interestingly, t6322016 matched the predicted precursors of novel miRNA candidates s391130a and s391130b, and those two were reported as antisense miRNA candidates as well (Zhang et al., 2012). Either s391130 or t6322016 might be a genuine miRNA resulting from 301078 to 301178 nt of Scaffold 352 (Table S1). Identification of additional novel miRNAs will facilitate genome annotation, miRNA clustering analysis on genome scaffolds and examination of closely resided genes to various miRNA loci.

We previously identified conserved *M. sexta* miRNAs with or without precursors (Zhang et al., 2012). There are two new conserved miRNA variants without precursors in the current dataset: miR-281 (ACUGUCAUGGAGUUGCUCUCUU) and miR-305 (AUUGUACUUCAUCAGGUGCUCU). We have normalized miRNA reads based on total read numbers of each library (Table 3 and Table S2) and Table 3 also includes novel miRNAs.

3.3. Certain miRNA* strands maintained at considerable levels

In the past, we proposed that certain miRNA star strands present at substantial levels may manipulate target gene expression and that two strands derived from a single miRNA precursor may regulate different targets (Zhang et al., 2014). For example, mse-miR-8* level fluctuates in fat body and hemocytes upon immune challenge and potentially regulates transcripts different from mse-miR-8 targets. mse-miR-8* is abundant in the current dataset. We have also found the star strands of mse-miR-9a, -9b, -10a, -14, -31, -71, -281, -308, -965 and -6097 were more abundant than their corresponding mature strands (Table 3). Three of them (mse-miR-31*, -281*, and -965*) were reported before (Zhang et al., 2012, 2014). Their precursors may favorably load the star strands into RISC. mse-miR-6097 and -6097*, first identified at low levels in the development series (Zhang et al., 2012), were much higher in the three tissues, especially hemocytes. Although mse-miR-9a* and -9b* were reported at levels similar to the mature strands (Zhang et al., 2012, 2014), it is unclear why mse-miR-9a*, -9b*, -10a*, -14*, -71* and -308* were remarkably more abundant in this dataset. It is worth noting that 5p- or 3p-arm miRNA dominant usage can be altered by the disease status: some prefer 5p-arms in normal tissue while others prefer 3p-arms in tumor tissue (Li et al., 2012b). However, different bacterial pathogens stimulated similar immune genes in the honeybee (Lourenco et al., 2013). There is no evidence supporting that insect miRNAs differentially react with different killed pathogens. The shorter treatment time and simpler pathogen combination may be related to the fact those six star strands were maintained at substantially higher levels. Differences in library construction procedures may also contribute to the higher abundances of miRNA*s since in the previous *M. sexta* studies small RNA libraries were constructed before they were delivered for sequencing (Zhang et

al., 2012, 2014). Therefore, the current dataset might be less consistent with the previous ones.

3.4. Abundances of M. sexta miRNAs in fat body, hemocytes and midgut

To examine expression patterns, we focused on the *M. sexta* miRNAs with identified precursors. After removing those with fewer than 10 normalized reads per million in each tissue, we categorized the remaining 102 miRNAs or miRNA*s into eight clusters based on K-means clustering (Fig. 3). After a closer examination of their normalized abundances, we organized the eight clusters into four groups. The first four clusters (group A) represented the 57 with higher abundances in hemocytes (Fig. 3A) – mse-miR-929b and -279c were also preferentially expressed in fat body. The next two clusters (group B) contained 27 entries preferentially expressed in fat body. mse-miR-100, -279b, -279d, -306 and t4742895* also exhibited high abundances in hemocytes; mse-miR-277 and -9a* showed expression preference in midgut as well. One cluster (group C) represented the nine preferentially expressed in midgut except mse-miR-2755* (Fig. 3C). The last cluster (group D) had seven highly expressed in both fat body and midgut (Fig. 3D) and two (mse-miR-283 and -283*) preferentially expressed in midgut only (Table 3). In summary, 36, 62 and 19 of the 102 miRNAs or miRNA*s were preferentially expressed in fat body, hemocytes and midgut, respectively.

3.5. miRNAs potentially targeting tissue-specific transcripts in fat body, hemocytes and midgut

Even though the preferential miRNA(*) groups were established based only on three tissues, that does not exclude their possible regulatory roles in specific tissues, especially when they are highly abundant. Therefore, it is intriguing to investigate what genes might be regulated in those tissues. From RNA-Seq data of 52 libraries of brain, fat body, midgut, muscle, Malpighian tubules, testes and ovary at various developmental stages, we identified 284 and 485 transcripts specifically expressed in day 1, 5^{th} instar larval fat body and midgut, respectively. Because hemocytes were not included in those 52 libraries, we selected and improved eleven hemocyte-specific transcripts based on the result from a previous transcriptome study (Zhang et al., 2011). Since most miRNAs recognize target mRNAs in the 3′-UTR, we used these regions from the tissue-specific transcripts to predict target sites of the preferential miRNAs in the corresponding tissues.

In the 3′ UTRs of hemocyte-specific transcripts for aminoacylase, hemolectin, HP1, IML-3a, IML-3b, lacunin, lectin, proPO-1, proPO-2, serpin 2 and SR-C like protein, we searched putative binding sites of the 62 miRNAs preferentially expressed in hemocytes. mse-miR-11*, t3301296, t3301296 and mse-miR-6093* potentially target aminoacylase, IML-3a, lacunin and serpin 2 transcripts, respectively (Table 4). Lectin and proPO-1 transcripts contained recognition sites of several miRNAs. MicroRNAs mse-miR-6093*, -6096-1, -6096-2, -6096-3 and t3301296 were identified as novel miRNAs (Zhang et al., 2012). t3301296 potentially regulates both IML-3a and lacunin, two arms of the mse-miR-11 precursor may regulate different targets (Table 4), and mse-miR-11, -190 and -308 may regulate proPO-1 (Zhang et al., 2014). While mse-miR-308 was preferentially expressed in fat body, we excluded mse-miR-bantam* because of its extreme scarcity. Thus,

by examining miRNA levels and tissue specificity, we can narrow down putative target lists and provide guidelines for functional verification.

Using 166 fat body- and 174 midgut-specific transcripts along with the 36 and 19 preferential miRNAs, we predicted recognition sites in the 3′-UTRs. Among the 166 transcripts in fat body, 62 may be involved in carbohydrate, lipid, amino acid, or xenobiotic metabolism and 19 in innate immunity (Table 5). Similarly, 82 of the 174 transcripts in midgut, involved in the aforementioned metabolism, are possibly regulated by the 19 miRNAs preferentially expressed in the same tissue (Table 6).

4. Discussion

4.1. Potential miRNA regulation of metabolic processes

After further examination of the fat body- and midgut-specific transcripts, we found the ones encoding proteins involved in electron transport and metabolism of carbohydrates, lipids, hormones, amino acids, and xenobiotics. Except for mse-miR-281*, -92b*, and -279b, all 36 fat body- and 19 midgut-preferential miRNAs had at least one possible target for these physiological processes. In the following discussion, we included potential regulatory miRNAs in the parentheses next to the transcript names.

4.1.1. Carbohydrate metabolism—There were five fat body and three midgut transcripts involved in carbohydrate degradation or synthesis. Brain chitinase and chia (mse-miR-79) and α-amylase (mse-miR-283) may hydrolyze the polysaccharides. Phosphonenolpyruvate synthase (mse-miR-316, -9571a, -281*) is a member of the glycolytic pathway. Trehalose, a major carbohydrate in insect hemolymph, is moved into cells by trehalose transporter Tret1 (mse-miR-2763, -iab-4). Glycogen synthase (mse-miR-10a, -12, -252, -2763, -8*), trehalose-6-phosphate synthase (mse-miR-1, -8*), and UDP-glucose pyrophosphatase (mse-miR-263b, -277, -306, -2763, -2768) in fat body and mannose-1-phosphate-guanylyltransferase (mse-miR-1) in midgut synthesize carbohydrates. Interestingly, mse-miR-1 and -8* may each regulate two transcripts. Meanwhile, mse-miR-2763 had recognition sites on 3′-UTRs of Tret1, glycogen synthase and UDP-glucose pyrophosphatase, suggestive of a role in trehalose uptake for storage in the form of glycogen.

Pentose phosphate pathway is crucial for the carbohydrate conversion. One midgut- and eight fat body-specific transcripts encode enzymes either in the pathway or providing pathway intermediates. They are: 6-phosphogluconate dehydrogenase (mse-miR-1, -282), 6-phosphogluconolactonase (mse-miR-282, t4742895), fructose-biphosphate aldolase (mse-miR-2763), phosphorglucomutase (mse-miR-10a*), phosphoribosyl pyrophosphate synthetase (mse-miR-1), transaldolase (mse-miR-277, -2763), *L*-xylulose reductase (mse-miR-9a*, -9b*, t4742895*), galactokinase-like protein (mse-miR-8*), and glucose dehydrogenase (mse-miR-137, -263b, -9a*). mse-miR-1, -282, -2763 and -9a* could each regulate two transcripts for the pathway members. Moreover, mse-miR-1, -277, -263b, -2763 and -8*, as potential regulators of carbohydrate conversion, may target genes in carbohydrate synthesis

4.1.2. Lipid metabolism—We found fat body-specific transcripts coding for proteins involved in fatty acid synthesis and lipid transport. Acetyl-CoA carboxylase (mse-miR-263b, -iab-4), ATP citrate lyase (mse-miR-10a, -277, -989), elongase (mse-miR-12, -79, -2763, -2768, -let-7a, -8*), fatty acid synthase (mse-miR-92b, -2763), long chain fatty acid elongase (mse-miR-1, -92a, -277, -281, -308), acyl-CoA Δ9 desaturase (m.106622) (mse-miR-2768), and acyl-CoA Δ9 desaturase (m.46170) (mse-miR-263a) participate in fatty acid synthesis. mse-miR-277, -2763, and -2768 may each regulate two targets. Acetyl-CoA carboxylase catalyzes the rate-limiting step of fatty acid synthesis and, thus, mse-miR-263b and -iab-4 may contribute to the rate modulation. Transcripts of fatty acid synthase contain recognition sites of mse-miR-92b and -2763 in the 3′-UTR. Awaiting future analysis is which one(s) of the four miRNAs (92b, 263b, iab-4 and 2763) are important to control fatty acid synthesis. Fat body is the main storage site for acylglycerols; adipokinetic hormone (AKH) induces the conversion of triacylglycerols to diacylglycerols for transportation to other tissues. Fat body-specific transcripts for the AKH receptor (mse-miR-263a, -iab-4, -8*) and its potential regulatory miRNAs should be tested for AKH binding. We also found two transcripts in fat body for lipid transport, apolipophorins (mse-miR-308) and apolipoprotein of lipid transfer particle III (mse-miR-2763, -2768).

In contrast, midgut-specific transcripts are responsible for acylglycerol hydrolysis and β-oxidation. Lipase (mse-miR-1), LPP1 (mse-miR-283), pancreatic lipase (mse-miR-137, -6094) and lysosomal acid lipase (mse-miR-263b, -9571b) take part in acylglycerol hydrolysis; acyl-CoA dehydrogenase (mse-miR-263a), enoyl-CoA hydratase (mse-miR-137) and enoyl-CoA isomerase (mse-miR-263a) in fatty acid β-oxidation. Since mse-miR-263a potentially regulates AKH receptor, acyl-CoA dehydrogenase, and enoyl-CoA isomerase, it is possible that this miRNA plays a significant role in fatty acid catabolism.

4.1.3. TCA cycle and electron transport chain and ATPases—TCA cycle is crucial for energy production and intermediate conversion. One fat body- and four midgut-specific transcripts are found: malate dehydrogenase (mse-miR-1, -263a, -278), citrate synthase (mse-miR-9a*), isocitrate dehydrogenase (m. 30761) (mse-miR-137, -277, -9571b), isocitrate dehydrogenase (m. 61421) (mse-miR-283), and succinyl-CoA ligase β chain (mse-miR-316). Among them, isocitrate dehydrogenase is important to regulate the whole TCA cycle and, therefore, it is interesting to test which one of the two transcripts encodes TCA isocitrate dehydrogenase and what miRNAs may regulate it. Reducing equivalents are needed for the respiratory chain to cause ATP synthesis while the malate-aspartate shuttle can transport cytosolic NADH into mitochondria. The midgut-specific transcripts of cytosolic malate dehydrogenase (mse-miR-137, -283), together with malate dehydrogenase, is an important component of the shuttle. The two enzymes may be regulated by different miRNAs in terms of enzyme expression levels. Cytochrome b5 (mse-miR-10a, -281, -316) in both fat body and midgut and cytochrome c homolog (mse-miR-281*) in midgut are members of the electron transport chain. There were 9 midgut transcripts encoding for ATP synthase/ATPases, but those were the vacuolar type which is not associated with the mitochondrial ATPases. Nevertheless, it is intriguing that mse-miR-1 had predicted target sites in seven 3′-UTRs of those nine transcripts. Recent studies found that although miRNAs are encoded by nuclear genes, certain miRNAs can accumulate in

mammalian mitochondria and components of miRNA machinery were detected there (Li et al., 2012a). While there is no evidence that insect miRNAs also accumulate in mitochondria to regulate mitochondrial activity, we hypothesize insect mitochondria have miRNA regulatory machinery as well. We found four fat body- and seven midgut-specific transcripts encoding mitochondrial proteins potentially regulated by miRNAs (Table 7). It would be interesting to verify which miRNAs are enriched in insect mitochondria to associate with their targets.

4.1.4. Amino acid metabolism—We found fat body-specific transcripts of amino acid synthases and other enzymes for Gly, Ser, Thr and Met metabolism, including Asn synthase (mse-miR-8, -282, -2763, t4742895*), Cys synthase (mse-miR-277), Gly cleavage system h protein (mse-miR-92b), Gly cleavage system p protein (mse-miR-12), Asn tRNA synthetase (mse-miR-277), D-3-phosphoglycerate dehydrogenase (mse-miR-92b, -308), Gly *N*-methyltransferase (mse-miR-12, -92b, -277 and -282), phosphatidylserine decarboxylase (mse-miR-308) and phosphoserine phosphatase (mse-miR-277). D-3-phosphoglycerate hydrogenase is the rate limiting step for Ser synthesis. mse-miR-92b and 308 may regulate three (D-3-phosphoglycerate dehydrogenase, glycine cleavage system h, and glycine N-methyltransferase) and two (D-3-phosphoglycerate hydrogenase and phosphatidylserine decarboxylase) in glycerine, serine and threnoine metabolic processes, respectively. mse-miR-12 and 277 were two other interesting candidates because they each potentially regulate two transcripts in Gly, Ser and Thr metabolism. For Met metabolism, there were two transcripts encoding hemocysteine-S-methyltransferase, m. 156992 (mse-miR-iab-4, -9a*, -9b*) and m.78459 (mse-miR-2763).

We found a fat body transcript, kynurenine formamidase (mse-miR-let-7a), and a midgut transcript, kynureninase (mse-miR-283, -316, -9571b), for tryptophan metabolism. Two midgut transcripts, isovaleryl-CoA dehydrogenase (mse-miR-10a and -316*) and methylcrotonoyl-CoA carbohylase 1α (mse-miR-10a* and -750*), are involved in Leu, Ile and Val metabolism. The 5p- or 3p-arm of mse-miR-10a precursor may regulate one of the two transcripts, implying that mse-miR-10a gene is important for Leu, Ile and Val metabolism. The conversion of amino groups into uric acid is important for disposal of excessive nitrogen in insects and there were four transcripts involved, branched-chain amino acid aminotransferase (mse-miR-33, -929, -2763, -2768 and -9a*), nitrilase (mse-miR-263a), amidase (mse-miR-263b), and aminoacyalase-1 (mse-miR-283).

4.1.5. Xenobiotic metabolism—There were five transcripts for cytochrome P450s and four transcripts for glutathione S-transferases, which are significant for xenobiotic metabolism in insects. mse-miR-9571b, a novel miRNA, may regulate three glutathione S-transferase transcripts; mse-miR-316* could recognize two glutathione S-transferases and one cytochrome P450. We also found aldehyde oxidase-2 (mse-miR-10a*) for cytochrome P450 oxidation and three enzymes involved in glutathione metabolism, γ-glutamyl cyclotransferase like (mse-miR-8*), γ-glutamyltransferase (mse-miR-2763, -278*) and lactoylglutathione lyase (mse-miR-9a*, -9b*, -750*). RNA interference has recently been utilized to affect expressions of cytochrome P450s, esterases or cadherin proteins to reduce insecticide resistance (Tang et al., 2010). Upon validation, this knowledge might be used to

affect insecticide resistance via specific miRNAs. Last but not the least, one fat body transcript for ABC transporter (t4742895) and one midgut transcript amino-peptidase N-11 (mse-miR-283) are potentially involved in the resistance to Bt toxin (Gahan et al., 2010; Likitvivatanavong et al., 2011).

4.1.6. Hormonal control—Ecdysteriods and juvenile hormones (JHs) are important lipid hormones to regulate various physiological processes in insects. We identified two fat body transcripts, JH epoxide hydrolase (mse-miR-100) and JH esterase (mse-miR-92a, -92b, -277, -929 and -let-7a) for JH inactivation. We also found a fat body transcript for ecdysone oxidase (mse-miR-12) and a midgut transcript for 3-hydroecdysone-3α-reductase (mse-miR-281, -316 and -283*) involved in ecdysone inactivation. Binding proteins of hemolymph JH (mse-miR-33, -2763, -2768) and cytosolic JH (mse-miR-9571a) were preferentially expressed in fat body and midgut, respectively. Since JH is not synthesized in midgut, it is interesting that one midgut specific transcript encodes FAMeT (mse-miR-283). The seven aforementioned transcripts related to hormonal control are possibly regulated by different miRNAs which manipulate the target gene expression.

4.2. Possible correlation between immunity and metabolism

By examining potential regulatory pairs of tissue-preferential miRNAs and -specific transcripts, we found miRNAs that may regulate genes for metabolic enzymes. This might explain why miRNAs are dysregulated in response to environmental stresses such as freezing and starvation, when hypo-metabolism happens. In *T. castanuem*, levels of five miRNAs arose while those of 22 miRNAs decreased upon starvation. Out of those 27 changed, we found seven conserved miRNAs (miR-1, -8, -79, -100, -279c, -279d and -let-7a) could target metabolic genes. These miRNAs were down-regulated in *T. castanuem* after starvation. Meanwhile, out of the 33 fat body preferential miRNAs targeting metabolic gene expression, levels of 18 (mse-miR-1, -8, -10a, -12, -33, -100, -252, -263a, -279c, -279d, -282, -306, -308, -989, -2763, -let-7a, -8*, -9b*) decreased and levels of 3 (mse-miR-92b, -277 and -iab-4) increased in *M. sexta* fat body after the immune challenge (Zhang et al., 2014). Thus these 21 miRNAs may correlate metabolism and systematic immune responses.

5. Conclusions

In this finale of our tripartite series, deep sequencing of the small RNAs from tissues under different conditions yielded a more extensive list of *M. sexta* miRNAs. Comparison of the normalized reads revealed miRNAs preferentially expressed in the tissues. Tethered with tissue-specific transcripts in fat body and midgut, we identified putative regulatory pairs of miRNAs and transcripts of metabolic enzymes. The initial data and premises help us to rationalize why miRNAs are dysregulated under stresses and how they may co-regulate metabolism and immunity. Along with the development and immunity profiles, we have analyzed experimental data to uncover a miRNA repertoire in the genome of this model insect, which fluctuates in tissues of different immune states at several life stages. After validating their targets in future studies, we can better appreciate the regulatory roles of miRNA in various insect physiological processes.

Supplementary Material

Refer to Web version on PubMed Central for supplementary material.

Acknowledgments

The research was supported by National Institutes of Health Grant GM58634 (to HJ), and a start-up fund from Kunming University of Science and Technology (to YZ). Part of the computation for this project was performed at OSU High Performance Computing Center at Oklahoma State University supported in part through the National Science Foundation grant OCI-1126330. This article was approved for publication by the Director of the Oklahoma Agricultural Experiment Station and supported in part under projects OKLO2450 (to HJ). We also thank Manduca Genome Project for Genome Assembly 1.0, funded by Defense Advanced Research Projects Agency (Gary Blissard, Boyce Thompson Institute) and National Institutes of Health (Michael Kanost, Kansas State University).

References

Asgari S. Role of MicroRNAs in Insect Host-Microorganism Interactions. Front Physiol. 2011; 2:48. [PubMed: 21886625]

Baker KD, Thummel CS. Diabetic larvae and obese flies-emerging studies of metabolism in Drosophila. Cell Metab. 2007; 6:257–266. [PubMed: 17908555]

Chawla G, Sokol NS. MicroRNAs in Drosophila development. Int Rev Cell Mol Biol. 2011; 286:1–65. [PubMed: 21199779]

Choi IK, Hyun S. Conserved microRNA miR-8 in fat body regulates innate immune homeostasis in Drosophila. Dev Comp Immunol. 2012; 37:50–54. [PubMed: 22210547]

Courteau LA, Storey KB, Morin P Jr. Differential expression of microRNA species in a freeze tolerant insect, Eurosta solidaginis. Cryobiology. 2012; 65:210–214. [PubMed: 22765989]

Davalos A, Goedeke L, Smibert P, Ramirez CM, Warrier NP, Andreo U, Cirera-Salinas D, Rayner K, Suresh U, Pastor-Pareja JC, Esplugues E, Fisher EA, Penalva LO, Moore KJ, Suarez Y, Lai EC, Fernandez-Hernando C. miR-33a/b contribute to the regulation of fatty acid metabolism and insulin signaling. Proc Natl Acad Sci U S A. 2011; 108:9232–9237. [PubMed: 21576456]

Etebari K, Asgari S. Conserved microRNA miR-8 blocks activation of the Toll pathway by upregulating Serpin 27 transcripts. RNA Biol. 2013; 10:1356–1364. [PubMed: 23806890]

Etebari K, Hussain M, Asgari S. Identification of microRNAs from Plutella xylostella larvae associated with parasitization by Diadegma semiclausum. Insect Biochem Mol Biol. 2013; 43:309–318. [PubMed: 23352895]

Freitak D, Knorr E, Vogel H, Vilcinskas A. Gender- and stressor-specific microRNA expression in Tribolium castaneum. Biol Lett. 2012; 8:860–863. [PubMed: 22628099]

Gahan LJ, Pauchet Y, Vogel H, Heckel DG. An ABC Transporter Mutation Is Correlated with Insect Resistance to Bacillus thuringiensis Cry1Ac Toxin. Plos Genet. 2010; 6

Grabherr MG, Haas BJ, Yassour M, Levin JZ, Thompson DA, Amit I, Adiconis X, Fan L, Raychowdhury R, Zeng QD, Chen ZH, Mauceli E, Hacohen N, Gnirke A, Rhind N, di Palma F, Birren BW, Nusbaum C, Lindblad-Toh K, Friedman N, Regev A. Full-length transcriptome assembly from RNA-Seq data without a reference genome. Nat Biotechnol. 2011; 29:644–U130. [PubMed: 21572440]

Gunaratna RT, Jiang H. A comprehensive analysis of the Manduca sexta immunotranscriptome. Dev Comp Immunol. 2013; 39:388–398. [PubMed: 23178408]

Hakimi MA, Cannella D. Apicomplexan parasites and subversion of the host cell microRNA pathway. Trends Parasitol. 2011; 27:481–486. [PubMed: 21840260]

Hiruma K, Riddiford LM. Developmental expression of mRNAs for epidermal and fat body proteins and hormonally regulated transcription factors in the tobacco hornworm, Manduca sexta. J Insect Physiol. 2010; 56:1390–1395. [PubMed: 20361974]

Hyun S, Lee JH, Jin H, Nam J, Namkoong B, Lee G, Chung J, Kim VN. Conserved MicroRNA miR-8/miR-200 and its target USH/FOG2 control growth by regulating PI3K. Cell. 2009; 139:1096–1108. [PubMed: 20005803]

Li B, Dewey CN. RSEM: accurate transcript quantification from RNA-Seq data with or without a reference genome. Bmc Bioinformatics. 2011; 12

Li P, Jiao J, Gao G, Prabhakar BS. Control of mitochondrial activity by miRNAs. J Cell Biochem. 2012a; 113:1104–1110. [PubMed: 22135235]

Li SC, Liao YL, Ho MR, Tsai KW, Lai CH, Lin WC. miRNA arm selection and isomiR distribution in gastric cancer. Bmc Genomics. 2012b; 13

Likitvivatanavong S, Chen JW, Bravo A, Soberon M, Gill SS. Cadherin, Alkaline Phosphatase, and Aminopeptidase N as Receptors of Cry11Ba Toxin from Bacillus thuringiensis subsp. jegathesan in Aedes aegypti. Appl Environ Microb. 2011; 77:24–31.

Lourenco AP, Guidugli-Lazzarini KR, Freitas FCP, Bitondi MMG, Simoes ZLP. Bacterial infection activates the immune system response and dysregulates microRNA expression in honey bees. Insect Biochem Molec. 2013; 43:474–482.

Lyons PJ, Lang-Ouellette D, Morin P Jr. CryomiRs: towards the identification of a cold-associated family of microRNAs. Comp Biochem Physiol Part D Genomics Proteomics. 2013a; 8:358–364. [PubMed: 24212287]

Lyons PJ, Poitras JJ, Courteau LA, Storey KB, Morin P Jr. Identification of differentially regulated micrornas in cold-hardy insects. Cryo Letters. 2013b; 34:83–89. [PubMed: 23435712]

Marco A, Hui JH, Ronshaugen M, Griffiths-Jones S. Functional shifts in insect microRNA evolution. Genome Biol Evol. 2010; 2:686–696. [PubMed: 20817720]

Pauchet Y, Wilkinson P, Vogel H, Nelson DR, Reynolds SE, Heckel DG, ffrench-Constant RH. Pyrosequencing the Manduca sexta larval midgut transcriptome: messages for digestion, detoxification and defence. Insect Mol Biol. 2010; 19:61–75. [PubMed: 19909380]

Saeed AI, Sharov V, White J, Li J, Liang W, Bhagabati N, Braisted J, Klapa M, Currier T, Thiagarajan M, Sturn A, Snuffin M, Rezantsev A, Popov D, Ryltsov A, Kostukovich E, Borisovsky I, Liu Z, Vinsavich A, Trush V, Quackenbush J. TM4: a free, open-source system for microarray data management and analysis. Biotechniques. 2003; 34:374–378. [PubMed: 12613259]

Stanley D, Miller J, Tunaz H. Eicosanoid actions in insect immunity. J Innate Immun. 2009; 1:282–290. [PubMed: 20375586]

Tang T, Liu X, Qiu L. RNA interference and its applications on silencing of insecticide-resistant genes in insects. Cotton Science. 2010; 22:617–624.

Zhang S, Gunaratna RT, Zhang X, Najar F, Wang Y, Roe B, Jiang H. Pyrosequencing-based expression profiling and identification of differentially regulated genes from Manduca sexta, a lepidopteran model insect. Insect Biochem Mol Biol. 2011; 41:733–746. [PubMed: 21641996]

Zhang X, Zheng Y, Jagadeeswaran G, Ren R, Sunkar R, Jiang H. Identification and developmental profiling of conserved and novel microRNAs in Manduca sexta. Insect Biochem Mol Biol. 2012; 42:381–395. [PubMed: 22406339]

Zhang X, Zheng Y, Jagadeeswaran G, Ren R, Sunkar R, Jiang H. Identification of conserved and novel microRNAs in Manduca sexta and their possible roles in the expression regulation of immunity-related genes. Insect Biochem Mol Biol. 2014; 47:12–22. [PubMed: 24508515]

Zheng Y, Zhang W. Animal microRNA target prediction using diverse sequence-specific determinants. Journal of Bioinformatics and Computational Biology. 2010; 8:763–788.

Zou Z, Najar F, Wang Y, Roe B, Jiang H. Pyrosequence analysis of expressed sequence tags for Manduca sexta hemolymph proteins involved in immune responses. Insect Biochem Mol Biol. 2008; 38:677–682. [PubMed: 18510979]

Zuker M. Mfold web server for nucleic acid folding and hybridization prediction. Nucleic Acids Res. 2003; 31:3406–3415. [PubMed: 12824337]

Abbreviations

ABC transporter	ATP-binding cassette transporter
ACBP	acyl-CoA-binding protein

ADCY	adenylate cyclase
ADGF	adenosine deaminase-related growth factor
ADK	adenylate kinase
AKH	adipokinetic hormone
AMP	antimicrobial peptide
ARF	ADP-ribosylation factor
CCDC	coiled-coil domain-containing protein
CF	control fat body
CH	control hemocytes
CoA	coenzyme A
DsCAM	Down syndrome cell adhesion molecule
eIF	eukaryotic translation initiation factor
FAMeT	farnesoic acid *O*-methyltransferase
Fkbp	FK509 binding protein
FMO	flavin-dependent monooxygenase
FPKM	fragments per kilobase of transcript per million mapped reads
GP	gut protease
HP	hemolymph protease
HSP	heat shock protein
IF	induced fat body
IH	induced hemocytes
IML	immulectin
JH	juvenile hormone
LAP	leucyl aminopeptidase
LPP	lipid phosphate phosphohydrolase
LRR	leucine-rich repeat protein
MCT	monocarboxylate transporter
MFE	minimal free energy
MSBP	membrane steroid binding protein
nt	nucleotide
PABP	polyadenylate binding protein
PAP	prophenoloxidase activating proteinase

proPO	prophenoloxidase
RISC	RNA induced silencing complex
SCOT	succinyl-CoA: 3-ketoacid CoA transferase
serpin	serine proteinase inhibitor
SSR	signal sequence receptor
TCA cycle	tricarboxylic acid cycle
TF	transcription factor
UTR	untranslated region

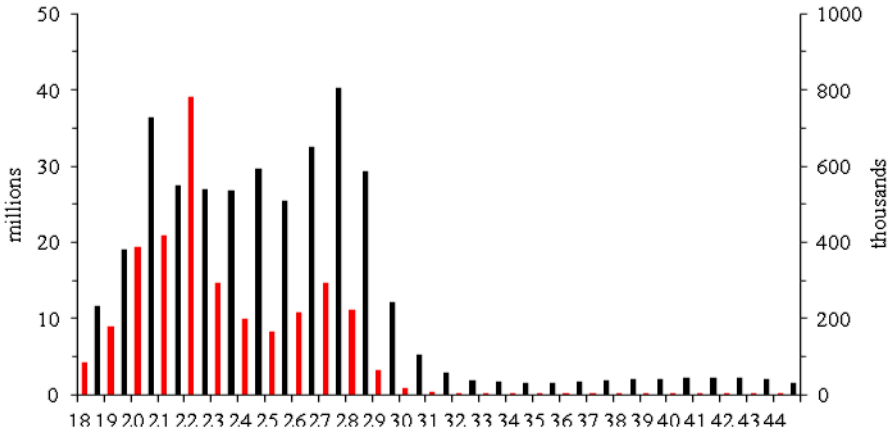

Fig. 1.

Length distributions of frequencies for total (*red bars, left y-axis*) and unique (*black bars, right y-axis*) reads in the three libraries combined.

Fig. 2.

Predicted fold-back structures of novel *M. sexta* miRNA precursors. Mature sequences are shown in red bold capital letters.

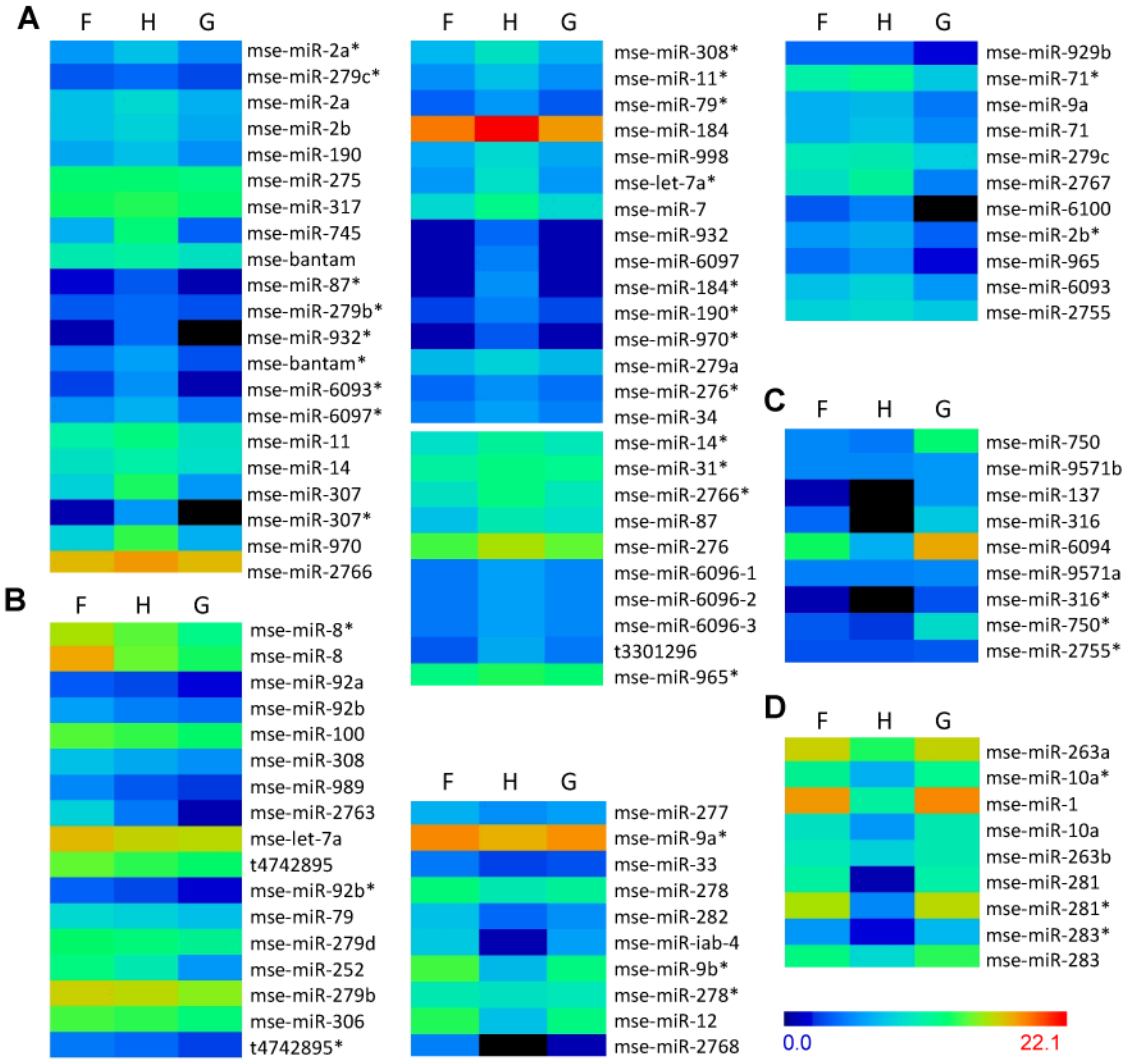

Fig. 3.

Eight clusters of *M. sexta* miRNA profiles with precursors identified. The color scale of $\log_2$NC is shown on the bottom right. $\text{Log}_2$0.5 (*i.e.* -1) is represented by black. F, H and G stands for fat body, hemocytes and midgut, respectively.

Table 1

Absolute read counts for different RNA categories*

Category	fat body		hemocytes		midgut	
	total	unique	total	unique	total	unique
noncoding RNAs	39,884,461	318,413	42,756,639	424,712	43,986,901	564,265
miRBase precursors	14,426,796	20,816	33,224,513	33,632	9,748,026	51,797
hemocyte, fat body & midgut ESTs	33,187,609	1,144,452	6,976,905	321,113	40,613,282	1,285,436
Cufflink transcripts	26,649,634	1,420,730	35,688,300	519,407	21,060,022	1,321,070
Repeats	8,405,172	103,019	4,519,342	139,428	12,297,243	196,431
Genome Assembly 1.0	40,295,140	1,766,651	42,846,338	786,176	35,183,741	1,606,036
Total	56,131,508	2,601,196	54,574,527	1,930,668	56,372,683	2,479,566

*Unique read numbers are ones after the removal of redundant reads.

Table 2

Newly discovered *M. sexta* novel miRNAs*

name	mature miRNA sequence	fat body		hemocytes		midgut		precursor MFE
		miR	miR*	miR	miR*	miR	miR*	
t357780	AAGGCGGUAAUUGUUGUUGAG	23	4	1	1	8	2	-30.2
t454580	AAUCGGACAAGCAGUGCGAACG	0	1	10	2	3	0	-34.8
t2290056	CGACCCUUGACAAAUCUUCUGA	3	4	12	4	5	4	-39.6
t3057689	GACAGAGAUUGUGGCAAGUCGUC	2	2	7	8	1	0	-29.1
t3301296	GAUGUACUGACUGUUUCAUCGC	75	0	598	2	147	0	-35.7
t4742895	UAUUAGAGUUCUGUGCUUCCUG	131975	157	66051	113	41738	47	-32.7

* Read numbers are absolute values from each library. The unit of precursor MFE is kcal/mol.

Table 3

Abundances of 71 conserved and 16 novel miRNAs with precursors identified*

Name	miRNA			miRNA*		
	fat body	hemocytes	midgut	fat body	hemocytes	midgut
mse-miR-1	307471	1976	392494			
mse-miR-1b	3	7	4			
mse-miR-2a	266	468	131	75	228	42
mse-miR-2b	229	400	113	71	113	16
mse-miR-7	525	3786	466	1	1	1
mse-miR-8	244823	25317	9301	59496	20768	3579
mse-miR-9a	128	182	27	425741	209874	356777
mse-miR-9b	6		1	16233	191	4575
mse-miR-10a	942	64	1401	2982	152	3372
mse-miR-10b		3				
mse-miR-10c		3				
mse-miR-11	1656	4572	873	58	218	47
mse-miR-12	11130	241	4453			
mse-miR-14	949	1787	665	709	2574	1099
mse-miR-31	2	2	2	2119	4558	3488
mse-miR-33	29	8	11	2	5	1
mse-miR-34	33	85	38	7	7	2
mse-miR-71	142	212	43	1731	3427	329
mse-miR-79	614	445	202	16	62	13
mse-miR-87	265	1502	767	4	13	2
mse-miR-92a	14	9	5			
mse-miR-92b	81	33	23	15	9	4
mse-miR-100	19743	13857	7546			
mse-miR-133	3		7			
mse-miR-137	2		70			
mse-miR-184	542406	4582805	311394	2	51	1

Name	miRNA			miRNA*		
	fat body	hemocytes	midgut	fat body	hemocytes	midgut
mse-miR-190	114	251	59	8	34	9
mse-miR-252	4830	1569	63			
mse-miR-263a	100055	9886	89284	2	1	4
mse-miR-263b	1262	447	1333	1		1
mse-miR-275	5880	7343	4927	1	6	2
mse-miR-276	16839	59742	23606	20	47	22
mse-miR-277	131	47	92	5	3	4
mse-miR-278	5731	1561	2541	1460	922	1176
mse-miR-279a	177	456	192	1		1
mse-miR-279b	104854	81110	40043	13	21	10
mse-miR-279c	1239	1431	346	13	21	9
mse-miR-279d	7474	5666	2880	5	7	
mse-miR-281	2228	1	1910	61841	41	79371
mse-miR-282	240	18	53	9	1	2
mse-miR-283	4314	473	11891	63	5	171
mse-miR-285		1				
mse-miR-306	16657	12512	5589			
mse-miR-307	374	9890	75	1	60	
mse-miR-308	263	102	52	163	896	139
mse-miR-316	18		309	1		11
mse-miR-317	8454	10567	6485	3	3	1
mse-miR-745	137	5127	16			
mse-miR-750	46	26	6192	12	6	648
mse-miR-929		1	1			
mse-miR-929b	18	18	5	1		
mse-miR-932	2	18	1	2	19	
mse-miR-965	22	56	5	4803	10406	6723
mse-miR-970	460	13584	127	2	12	1

Insect Biochem Mol Biol. Author manuscript; available in PMC 2015 July 01.

Name	miRNA			miRNA*		
	fat body	hemocytes	midgut	fat body	hemocytes	midgut
mse-miR-981-1	1		2			
mse-miR-981-2	1		2			
mse-miR-989	45	12	6			
mse-miR-993	1					
mse-miR-998	105	520	100			
mse-miR-2755	411	558	275	11	11	13
mse-miR-2763	433	30	1			
mse-miR-2765	6	3	3			
mse-miR-2766	188347	321433	159054	868	4978	1222
mse-miR-2767	994	2413	32			
mse-miR-2768	33		1			
mse-miR-2796			4			
mse-miR-3286	1			2		1
mse-miR-3338	2					
mse-miR-6093	200	419	61	8	58	2
mse-miR-6094	8653	145	228818			
mse-miR-6096-1	27	87	40	1	2	1
mse-miR-6096-2	27	87	40	1	2	1
mse-miR-6096-3	27	87	40	1	2	1
mse-miR-6097	2	32	1	47	125	23
mse-miR-6100	13	35		1	2	
mse-miR-9570	2	2	3			
mse-miR-9571a	34	35	46		1	
mse-miR-9571b	46	45	72			1
t357780	4		1	1		
t454580		2	1			
t2290056	1	2	1	1	1	1
t3057689		1			1	

Name	miRNA			miRNA*		
	fat body	hemocytes	midgut	fat body	hemocytes	midgut
t3301296	13	110	26			
t4742895	23512	12103	7404	28	21	8
mse-bantam	1362	2291	1009	29	89	10
mse-miR-iab-4	288	2	90			
mse-let-7a	177249	94886	79507	70	791	62

*Abundances are shown as normalized reads per million (NRPM). Numbers are blank for those either non-detectable or with normalized values below 0.5.

Table 4

Predicted hemocyte-specific targets

gene	miRNA
aminoacylase	mse-miR-11*
IML-3a	t3301296
lacunin	t3301296
lectin	mse-miR-11, 6096-1, 6096-2, 6096-3
proPO-1	mse-miR-11, 190, bantam*
serpin 2	mse-miR-6093*

Table 5

Predicted fat body-specific targets *

miRNA	putative targets
mse-miR-1	2-deoxyglucose-6-phosphate phosphatase, 6-phosphogluconate dehydrogenase, ADCY type 9, AMP deaminase 2, eIF4A, Innexin, malate dehydrogenase, Na(+)/H(+) hydrogen antiporter 1, PABP-interacting protein 1, phospho- ribosyl pyrophosphate synthetase, phosphoribosylformylglycinamidine synthase, 5-aminoimidazole-4-carboxamide ribonucleotide formyltransferase, Kelch-like protein 10, long chain fatty acid elongase, sugar transporter (m.65628), sugar transporter (m. 197206), trehalose-6-phosphate synthase
mse-miR-8	alanine-glyoxylate aminotransferase, Asn synthetase, endothelin converting enzyme, karmoisin, Na(+)/H(+) hydro-gen antiporter 1, phosphoribosylformylglycinamidine synthase, prenyl-dependent CAAX metalloprotease, cuticle protein (m. 22182), mitochondrial carrier protein, procollagen-lysine-2-oxoglutarate 5-dioxygenase, salivary purine nucleosidase, seminal fluid protein CSSFP048, serine protease-like protein 4, sugar transporter 4
mse-miR-10a	ATP citrate lyase, Cameo2, cytochrome B5, eIF4A, fusilli isoform G, glycogen synthase, NIPSNAP protein, PAP1, Phe hydroxylase, hypoxia inducible factor 1, Ras-related protein rab-39b-like, SLY-1 homolog, syndecan, UDP-glycosyltransferase (m.51342)
mse-miR-12	ADCY type 9, Cameo2, carbonic anhydrase, DNA supercoiling factor, elongase, FAD-dependent oxidoreductase, glycine cleavage system P, glycine N-methyltransferase like, glycogen synthase, HP6, plexin A, protein disulfide isomerase, 2-oxoacid dehydrogenases acyltransferase, ecdysone oxidase, serpin 3, sugar transporter (m.154929), Tolloid-like protein 2, translocation protein SEC62
mse-miR-33	alanine-glyoxylate aminotransferase, AMP deaminase 2, branched-chain AA aminotransferase, cytochrome P450 (m.17726), hemolymph JH binding protein, HP21, immunolectin A, Na(+)/H(+) hydrogen antiporter 1, ovary C/EBPg TF, prenyl-dependent CAAX metalloprotease, Ras-related protein rab-39b-like, SLY-1 homolog
mse-miR-79	adenosylhomocysteinase, brain chitinase and chia, cytochrome P450 (m.236105), disulfide isomerase, eIF4A, elongase, IML-3, innexin, karmoisin, Na(+)/H(+) hydrogen antiporter 1, purine nucleoside phosphorylase, serpin 4
mse-miR-92a	ADCY type 9, α-mannosidase II, colmedin, dorsoventral patterning protein tolloid, glutathione S-transferase Ω3, guanine deaminase, JH esterase, molybdopterin synthase catalytic subunit 2, nicotinamide riboside kinase 1, Phe hydroxylase, 5-aminoimidazole-4-carboxamide ribonucleotide formyltransferase, long chain fatty acid elongase, secreted peptide 30, seminal fluid protein CSSFP048, sugar transporter (m.154929)
mse-miR-92b	α-mannosidase II, D-3-phosphoglycerate dehydrogenase, fatty acid synthase, glutathione S-transferase Ω3, glycine cleavage system h, glycine N-methyltransferase like, HSP60, IML-3, JH esterase, lipid storage droplet protein, molybdopterin synthase catalytic subunit 2, myostatin, nicotinamide riboside kinase 1, ovary C/EBPg TF, S-adenosylmethionine synthase, seminal fluid protein CSSFP048, SLY-1 homolog, sugar transporter (m.154929)
mse-miR-100	HSP60, JH epoxide hydrolase like, mitochondrial ornithine transporter, Na(+)/H(+) hydrogen antiporter 1, S-adenosylmethionine synthase
mse-miR-252	eIF4A, endothelin converting enzyme, gloverin, glycogen synthase, karmoisin, Na(+)/H(+) hydrogen antiporter 1, nicotinic acetylcholine receptor subunit α, purine nucleoside phosphorylase, serpin 13, sugar transporter (m.197206), Tolloid-like protein 2
mse-miR-263a	acyl-CoA Δ9 desaturase (m.46170), adipokinetic hormone receptor, β-hexosaminidase (m.22649), Cameo2, cGMP-dependent protein kinase, collagen α1(IV) chain, endothelin converting enzyme, glutathione S-transferase Ω3, innexin, malate dehydrogenase, nicotinic acetylcholine receptor subunit α, purine nucleoside phosphorylase, seminal fluid protein CSSFP011 isoform 1, seminal fluid protein CSSFP048, serpin 3, serpin 4, syndecan, TNFSF13, Xanthine dehydrogenase
mse-miR-263b	acetyl-CoA carboxylase, β-hexosaminidase (m.22649), DNA supercoiling factor, DsCAM, eIF4A, IML-3, metalloprotease, UDP-glucose pyrophosphatase
mse-miR-277	AMP deaminase 2, Asn-tRNA synthetase, ATP citrate lyase, chondroitin 4-sulfotransferase, Cys synthase, eIF4A, endothelin converting enzyme, glycine N-methyltransferase like, HSP60, JH esterase, karmoisin, multiple coagulation factor deficiency protein 2 like, NIPSNAP protein, PABP-interacting protein 1, phosphoserine phosphatase, Pro-4-hydroxylase α subunit, aldehyde dehydrogenase (m.175855), f-spondin, hypoxia inducible factor 1, long chain fatty acid elongase, procollagen-lysine-2-oxoglutarate 5-dioxygenase, tyrosine protein kinase, Ras-related protein rab-39b-like, S-adenosyl-Met synthase, serpin 4, transaldolase, UDP-glucose pyrophosphatase
mse-miR-278	malate dehydrogenase, Na(+)/H(+) hydrogen antiporter 1, UDP-glycosyltransferase (m.150628)
mse-miR-279b	collagen α1(IV) chain, S-adenosyl-Met decarboxylase, sugar transporter (m.197206)
mse-miR-279c	ADCY type 9, collagen α1(IV) chain, nicotinic acetylcholine receptor subunit α, mitochondrial solute carrier, S-adenosyl-Met decarboxylase
mse-miR-279d	ADCY type 9, collagen α1 (IV) chain, HP6, nicotinic acetylcholine receptor subunit α, MCT, S-adenosyl-Met decarboxylase, sugar transporter (m.197206)
mse-miR-281	Cameo2, cytochrome B5, eIF4A, long chain fatty acid elongase, SLY-1 homolog

miRNA	putative targets
mse-miR-282	6-phosphogluconate dehydrogenase, 6-phosphogluconolactonase, AMP deaminase 2, Asn synthetase, Gly N-methyltransferase like
mse-miR-306	Cameo2, FMO3, H/ACA ribonucleoprotein complex subunit 3, LAG1 longevity assurance like protein 6, metalloprotease, hypoxia inducible factor 1, Kelch-like protein 10, Na-dependent phosphate transporter, UDP-glucose pyrophosphatase, UDP-glycosyltransferase (m.150628)
mse-miR-308	ADCY type 9, adenosylhomocysteinase, α-mannosidase II, apolipophorins, Cameo2, D-3-phosphoglycerate dehydrogenase, Mid1-interacting protein 1 like, multiple coagulation factor deficiency protein 2 like, Na(+)/H(+) hydrogen antiporter 1, nicotinamide riboside kinase 1, phosphatidylserine decarboxylase, plexin A, long chain fatty acid elongase, procollagen-lysine-2-oxoglutarate 5-dioxygenase, Scavenger receptor class B, serpin 4, Sparc, sugar transporter (m.154929), syndecan
mse-miR-929b	branched-chain AA aminotransferase, JH esterase, UDP-glycosyltransferase (m.150628)
mse-miR-989	ATP citrate lyase, β-hexosaminidase (m.22649), chordin, eIF4A, NADH cytochrome B5 reductase, NIPSNAP protein, plexin A, protein disulfide isomerase, Ras-related protein rab-39b-like, serpin 4
mse-miR-2763	adenosylhomocysteinase, α-mannosidase II, AMP deaminase 2, apolipoprotein of lipid transfer particle III, Asn synthetase, β-hexosaminidase (m.171987), β-hexosaminidase (m.22649), branched-chain AA aminotransferase, Cameo2, carbonic anhydrase, eIF4A, elongase, endothelin converting enzyme, o trehalose transporter Tret1, fatty acid synthase, fructose-bisphosphate aldolase, fusilli isoform G, γ-glutamyltransferase, glutathione S-transferase Ω3, glycogen synthase, hemolymph JH binding protein, HP6, IML-3, karmoisin, molybdopterin binding protein, Na(+)/H(+) hydrogen antiporter 1, PAP3, Phe hydroxylase, aldehyde dehydrogenase (m.190690), aldehyde oxidase (m.79792), hemicentin-1, homo-Cys S-methyltransferase (m.78459), serpin, Ras-related protein rab-39b-like, SLY-1 homolog, small HSP, syndecan, Tolloid-like protein 2, transaldolase, trypsin like proteinase, UDP-glucose pyrophosphatase, Xanthine dehydrogenase
mse-miR-2768	acyl-CoA Δ9 desaturase (m.106622), adenosylhomocysteinase, apolipoprotein of lipid transfer particle III, branched-chain AA aminotransferase, dihydropteridine reductase, elongase, fusilli isoform G, hemolymph JH binding protein, hemolymph protein, PABP-interacting protein 1, PAP1, Phe hydroxylase, plexin A, aldehyde dehydrogenase (m.175855), CRAL/TRIO domain-containing protein, cuticle protein (m.169920), sugar transporter (m.197206), UDP-glucose pyrophosphatase
t4742895	6-phosphogluconolactonase, ABC transporter, disulfide isomerase, eIF4A, Fkbp13, myostatin, cuticle protein (m.22182), SLY-1 homolog, Taurine catabolism dioxygenase
mse-let-7a	α-mannosidase II, eIF4A, elongase, fusilli isoform G, Glutathione S-transferase Ω3, JH esterase, karmoisin, kynurenine formamidase, serpin 4, small HSP
mse-miR-iab-4	acetyl-CoA carboxylase, adipokinetic hormone receptor, trehalose transporter Tret1, karmoisin, lebocin-like protein B, nicotinic acetylcholine receptor subunit α, phosphatidylethanolamine binding protein, prenyl-dependent CAAX metalloprotease, α-N-acetyl glucosaminidase, homo-Cys S-methyltransferase (m.156992), scavenger receptor class B, small GTP binding protein RAB8
mse-miR-8*	adipokinetic hormone receptor, α-mannosidase II, disulfide isomerase, elongase, galactokinase like, γ-glutamyl cyclotransferase like venom protein, glutathione S-transferase Ω3, glycogen synthase, Na(+)/H(+) hydrogen antiporter 1, PABP-interacting protein 1, trehalose-6-phosphate synthase
mse-miR-9a*	AMP deaminase 2, branched-chain AA aminotransferase, Cameo2, DNA supercoiling factor, eIF4A, hemicentin-like protein 2, hemolymph protein, lactoylglutathione lyase, L-xylulose reductase, purine nucleoside phosphorylase, homo-Cys S-methyltransferase (m.156992), procollagen-lysine-2-oxoglutarate 5-dioxygenase, small HSP, Tolloid-like protein 2
mse-miR-9b*	Cameo2, DNA supercoiling factor, eIF4A, Hemicentin-like protein 2, Hemolymph protein, HP21, Lactoylglutathione lyase, L-xylulose reductase, NIPSNAP protein, purine nucleoside phosphorylase, homo-Cys S-methyltransferase (m.156992), procollagen-lysine-2-oxoglutarate 5-dioxygenase, Tolloid-like protein 2
mse-miR-10a*	ADCY type 9, aldehyde oxidase 2, metalloprotease, molybdopterin synthase catalytic subunit 2, phosphogluco-mutase, f-spondin, tricarboxylate transport protein, TNFSF13, translocation protein SEC62
mse-miR-92b*	myostatin, Na(+)/H(+) hydrogen antiporter 1, neurotrimin, plexin A, purine nucleoside phosphorylase, taurine catabolism dioxygenase
mse-miR-278*	fusilli isoform G, γ-glutamyltransferase
mse-miR-281*	PAP1, cuticle protein (m.22182), hemicentin-1, serpin 4, small GTP binding protein RAB8
t4742895*	Asn synthetase, DsCAM, fusilli isoform G, hemolymph protein, L-xylulose reductase, Kelch-like protein 10, mitochondrial carrier protein

*If gene names are the same, the transcript IDs (m. number) were included in the parentheses.

Table 6

Predicted midgut-specific targets *

miRNA	putative targets
mse-miR-1	adenylsulfate kinase, calmodulin, copper transporter, HoxX, hydroxybutyrate dehydrogenase (m.24658), isochorismatase domain containing protein, lipase, mitochondrial succinate semialdehyde dehydro-genase, protein mesh, α-1,3-fucosyltransferase, glucocerebrosidase isoform 1, mannose-1-phosphate guanylyltransferase, selenoprotein M, vacuolar ATP synthase subunit S1, pyridoxal-phosphate dependent enzyme, pyridoxine 5′-phosphate oxidase, regucalcin, renin receptor like isoform 1, RING finger protein 181, serine protease (m.165170), sideroflexin, sterol carrier protein 2/3-oxoacyl-CoA thiolase, sugar transporter (m.45569), synaptobrevin, tetraspanin1, vacuolar ATP synthase 21 kDa proteolipid subunit, v-type proton ATPase subunit C, v-type proton ATPase subunit D, v-type proton ATPase subunit E, v-type proton ATPase subunit F, v-type proton ATPase subunit G
mse-miR-10a	adenylate cyclase, eIF2A, GP40, isovaleryl CoA dehydrogenase, metal transporter CNNM2 like, peripheral-type benzodiazepine receptor, protein canopy like, synaptic vesicle protein, SSR β subunit
mse-miR-137	4-nitrophenylphosphatase, ACBP, Acyltransferase, ADGF-like, Bombyrin precursor, CCDC, cytosolic malate dehydrogenase, enoyl CoA hydratase, glucose dehydrogenase, glutathione S-transferase 13, isocitrate dehydrogenase (m.30761), pancreatic lipase, prenyl-dependent CAAX metalloprotease, bhlhzip TF bigmax, carboxypeptidase A like, dipeptidyl peptidase, mitochondrial short-chain specific acyl-CoA dehydrogenase, zinc finger protein, pyroglutamyl peptidase 1, sugar transporter (m.222220), sugar transporter SWEET1, TPPP family protein, trypsin-like protease, v-type proton ATPase subunit D
mse-miR-263a	2-deoxyglucose-6-phosphate phosphatase, acyl-CoA dehydrogenase, cadherin, carboxypeptidase B, dimeric dihydrodiol dehydrogenase, enoyl CoA isomerase, MCT (m.228787), nitrilase, protein mesh, RING finger and WD repeat domain-containing protein 3, sugar transporter (m.45569)
mse-miR-263b	AMP dependent CoA ligase, ecdysoneless, glucose dehydrogenase, HSP90 β, metal transporter CNNM2 like, protein cueball, amidase, bhlhzip TF bigmax, cAMP-dependent protein kinase catalytic subunit, lysosomal acid lipase, pyroglutamyl peptidase 1, retinol dehydrogenase
mse-miR-277	2-hydroxyphytanoyl-CoA lyase, ACBP homolog, AMP dependent CoA ligase, bombyrin precursor, chorion b-ZIP TF, cytochrome P450 (m.45481), flavin reductase, HSP105, inorganic pyrophosphatase, isocitrate dehydrogenase (m.30761), maggie, mitochondrial succinate semialdehyde dehydrogenase, peripheral-type benzodiazepine receptor, phosphotriesterase like, prohibitin WPH, protein cueball, α-1,3-fucosyltransferase, carbonic anhydrase, pyroglutamyl peptidase 1, regucalcin, SCOT, Sel1 repeat-containing protein 1 like, serpin 15A, sphingolipid Δ4-desaturase, TPPP family protein, transporter (m.87506), v-type proton ATPase subunit B
mse-miR-281	3-dehydroecdysone-3alpha reductase, carboxypeptidase 3, CRAL-TRIO domain-containing protein, cytochrome P450 6AE32, eIF2A, glutamate receptor, inorganic pyrophosphatase, isochorismatase domain containing protein, LRR, NADPH cytochrome P450 reductase, serpin 15A
mse-miR-283	acyltransferase, adenylsulfate kinase, α-amylase, aminoacylase 1, aminopeptidase N-11, Bombyrin precursor, calmodulin isoform A, copper transporter, cytosolic malate dehydrogenase, ER lumen protein retaining receptor, FAMeT, fatty acid binding protein, glutamate receptor, GP40, hydroxysteroid dehydro-genase, isocitrate dehydrogenase (m.61421), kynureninase, LPP1, MSBP, peritrophic membrane chitin binding protein, alcohol dehydrogenase, cAMP-dependent protein kinase catalytic subunit, carbonic anhydrase, pyridoxine 5′-phosphate oxidase, SCP related protein, short chain type dehydrogenase (m.29729), sphingolipid Δ4-desaturase, sugar transporter (m.222220), synaptobrevin, trypsin alkaline D, trypsin-like protease, v-type proton ATPase subunit D
mse-miR-316	3-dehydroecdysone-3α reductase, Arg kinase, calmodulin isoform A, cytochrome b5, GP40, hatching enzyme like protein, hydroxybutyrate dehydrogenase (m.198924), kynureninase, LAP, mitochondrial cytochrome C oxidase subunit 6A, phosphoenolpyruvate synthase, alcohol dehydrogenase, regucalcin, SSR, succinyl-CoA ligase β chain, Toll9, TP53-regulated inhibitor of apoptosis 1-B
mse-miR-750	organic cation transporter (m.212782), Pap-inositol-1,4-phosphatase, sodium-bile acid co-transporter, V-type proton ATPase subunit B
mse-miR-6094	carboxyl cholinesterase, pancreatic lipase, peripheral-type benzodiazepine receptor, Ras family protein, short chain type dehydrogenase (m.29729), vacuolar ATPase subunit M9.7
mse-miR-9571a	2-deoxyglucose-6-phosphate phosphatase, ACBP, adrenodoxin, Bombyrin precursor, calcium-binding protein p22, copper transporter, cytosolic JH binding protein 36 kDa subunit, GP40, HoxX22, lipid storage droplet protein 2, mitochondrial carrier like, mitochondrial NADPH adrenodoxin oxidoreductase, neuro-peptide receptor A10, Pap-inositol-1,4-phosphatase, peptidyl-prolyl cis-trans isomerase, peroxisomal biogenesis factor 19, phosphoenolpyruvate synthase, bhlhzip TF bigmax, mitochondrial short-chain specific acyl-CoA dehydrogenase, Ras family protein, RGS-GAIP interacting protein GIPC, SCP related protein, sugar transporter SWEET1, transferrin3, trypsin-like protease, v-type proton ATPase subunit F
mse-miR-9571b	2-deoxyglucose-6-phosphate phosphatase, ACBP, adrenodoxin, Bombyrin precursor, B. mori glutathione-S-transferase 4, B. mori glutathione-S-transferase 5, calcium-binding protein p22, carbonyl reductase, chitin binding domain 3 protein, copper transporter, fatty acid binding protein, glutathione S-transferase 13, His-triad nucleotide binding protein 3, hydroxybutyrate dehydrogenase (m.24658), isocitrate dehydrogenase (m.30761), kynureninase, MCT (m.94739), mitochondrial carrier like, MSBP, Pap-inositol-1,4-phosphatase, peripheral-type benzodiazepine receptor, α-1,3-fucosyltransferase, bhlhzip TF bigmax, lysosomal acid lipase, RAB6-interacting golgin like, vacuolar ATP synthase subunit S1, pyroglutamyl peptidase 1,

miRNA	putative targets
	Ras family protein, SCP related protein, serine protease (m.46246), short chain type dehydrogenase (m.81137), sugar transporter SWEET1, synaptic vesicle glycoprotein 2B, synaptobrevin, transporter (m.78218), v-type proton ATPase subunit F
mse-miR-9a*	chitin binding domain 3 protein, citrate synthase, cytochrome P450 4M1, ecdysoneless, glucose dehydrogenase, HoxX, lactoylglutathione lyase, LRR, metal transporter CNNM2 like, methylmalonyl-CoA carboxyltransferase 12S subunit, organic cation transporter (m.57266), peroxisomal biogenesis factor 19, harmonin, SCP related protein
mse-miR-10a*	glutathione S-transferase 13, HoxX22, methylcrotonoyl-CoA carboxylase 1α, NADPH cytochrome P450 reductase, dipeptidyl peptidase, SSR β subunit
mse-miR-281*	cytochrome c-like, isochorismatase domain containing protein, phosphoenolpyruvate synthase, bhlhzip TF bigmax
mse-miR-283*	3-dehydroecdysone-3α reductase, eIF2A, O-acyltransferase, peroxisomal biogenesis factor 19, prenyl-dependent CAAX metalloprotease, bhlhzip TF bigmax, pyridoxal-phosphate dependent enzyme
mse-miR-316*	acetoacetyl-CoA thiolase, ARF, B. mori glutathione-S-transferase 4, cytochrome P450 6AE32, fatty acid binding protein, glutathione S-transferase 13, HoxX, innexin, isovaleryl CoA dehydrogenase, metal transporter CNNM2 like, ADK 3, regucalcin, retinol dehydrogenase, short chain type dehydrogenase (m.29729), v-type proton ATPase subunit C
mse-miR-750*	dimeric dihydrodiol dehydrogenase, lactoylglutathione lyase, methylcrotonoyl-CoA carboxylase 1α, NADPH cytochrome P450 reductase

* If gene names are the same, the transcript IDs (m. number) were included in the parentheses.

Table 7
Potential regulatory pairs of miRNAs and mitochondrial genes

Gene	miRNA
mitochondrial ornithine transporter	mse-miR-100
mitochondrial carrier protein	mse-miR-8, t4742895*
mitochondrial solute carrier	mse-miR-279c
tricarboxylate transport protein	mse-miR-10a*
adrenodoxin	mse-miR-9571a, 9571b
mitochondrial cytochrome C oxidase subunit 6A	mse-miR-316
mitochondrial NADPH adrenodoxin oxidoreductase	mse-miR-9571a
mitochondrial succinate semialdehyde dehydrogenase	mse-miR-1, 277
mitochondrial short-chain specific acyl CoA dehydrogenase	mse-miR-137, 9571a
SCOT	mse-miR-277
mitochondrial carrier like	mse-miR-9571a, 9571b